Journal of Membrane Science & Research

journal homepage: www.msrjournal.com

Research Paper

Performance of Chemically Modified TiO_2-poly (vinylidene fluoride) DCMD for Nutrient Isolation and Its Antifouling Properties

N.S. Mohd Yatim, K. Abd. Karim, O. Boon Seng*

School of Chemical Engineering, Engineering campus, Universiti Sains Malaysia, Seri Ampangan, 14300 Nibong Tebal, Penang, Malaysia

ARTICLE INFO

Received 2015-11-03
Revised 2015-12-23
Accepted 2015-12-29
Available online 2015-12-29

KEYWORDS

Membrane distillation (MD)
DCMD
Nanocomposite
Chemical modification
Biofouling

GRAPHICAL ABSTRACT

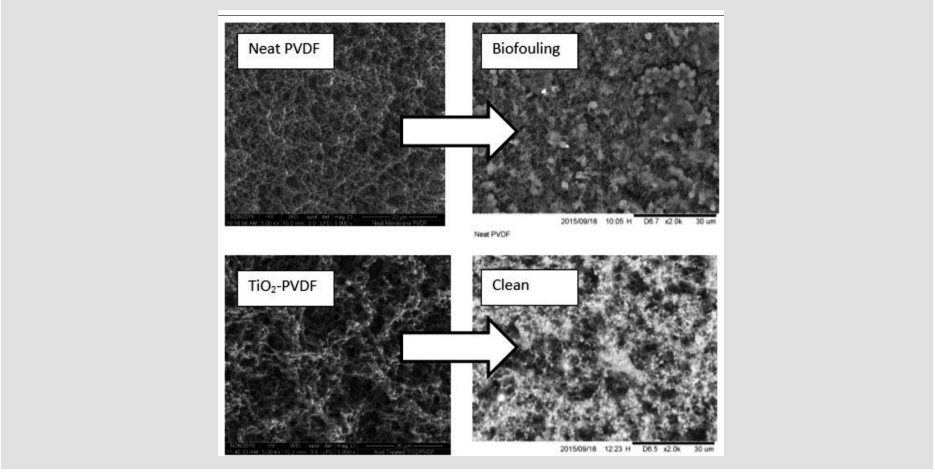

HIGHLIGHTS

- PVDF membrane with TiO_2 dosage shows significant antibacterial properties.
- Addition of untreated TiO_2 impair the membrane porosity and liquid entry pressure.
- Acid/alkali treated TiO_2 gave improved performance of the TiO_2-PVDF composite.

ABSTRACT

The surface properties of TiO_2-PVDF nanocomposite membranes were investigated by incorporating different chemically modified TiO_2 nanoparticles into the poly (vinylidene fluoride) (PVDF) matrix. The nanocomposite membranes were prepared via dual coagulation bath diffusion and the induced phase inversion method. The membrane surface morphologies were investigated by using SEM and AFM and related to the membrane surface energy via contact angle goniometry. The results showed that the average membrane surface pore sizes were increased with the addition of TiO_2 nanoparticles. Nonetheless, the contact angle measurements demonstrated that the hydrophobicity of nanocomposite membranes can be maintained even with the addition of hydrophilic TiO_2. This observation could be rationalized as surface roughness enhancement. The experimental results demonstrated that the initial flux of acid treated TiO_2 has both higher initial flux and high COD removal due to their induced surface roughness. The TiO_2-PVDF membranes were found to possess the significant bactericidal effect on B. Subtilis compared to the neat membrane even without the presence of UV light.

1. Introduction

In recent years, the incorporation of inorganic additives into polymeric materials to modify its performance has expanded remarkably for membrane separation. A variety of nanoparticles have been introduced to modify organic membranes, such as SiO_2 [1], Al_2O_3 [2], Fe_3O_4 [3] and TiO_2 [4, 5] with the common aims to enhance the performance of the membrane in terms of flux enhancement and antifouling properties. Among the nanoparticles, TiO_2 has received much attention because of its robust physical and chemical

* Corresponding author at: Phone: +6045996418; fax: +6045996908
E-mail address: chobs@usm.my (O. Boon Seng)

properties as well as its potential antifouling and antibacterial properties [6, 7]. Damodar and Rahimpour investigated the antibacterial properties of the membrane that was entrapped with TiO_2. The results indicated that the TiO_2 modified membrane under UV light had better bactericidal ability due to its photocatalytic property [6].

Poly(vinylidenefluoride) (PVDF) is one of the polymeric materials which is commonly used in membrane distillation (MD). Its wide application is due to the material excellence thermal, chemical, and oxidation resistances properties against corrosive chemicals such as acids, bases, oxidants and halogens [8, 9]. Furthermore, PVDF is a hydrophobic material which makes it a suitable candidate to be applied in MD due to its non-wetting properties. However, hydrophobic material usually has poor anti-organic/bio-fouling properties which impaired its applications and life span [10]. Therefore, a combination of synergistic bactericidal properties of TiO_2 nanoparticles and the hydrophobic nature of PVDF membranes offer its beneficial applications for wastewater treatment in membrane distillation mode.

One of the biggest issues with the TiO_2-PVDF nanocomposite membrane is that the addition of TiO_2 could change the membrane surface from hydrophobic to hydrophilic due to the presence of the hydroxyl group. While TiO_2 can improve the antifouling properties of the membrane due to its hydrophilic nature, it rendered the membrane with an unwanted higher surface energy not suitable for MD. A previous study by Li et al. showed that incorporating the unmodified Degussa P25 (21 nm particle size, 80% anatase) on the PES microfiltration membrane produces membranes with a higher hydrophilicity surface as well as better permeation performance [11]. On the other hand, Razmjou et al. turn the nanocomposite membrane into a superhydrophobic membrane by creating a hierarchical structure with multi-level roughness via depositing TiO_2 nanoparticles on the microporous PVDF membranes by means of a low temperature hydrothermal (LTH) process. The liquid entry pressure (LEPw) and water contact angle was increased from 120 kPa and 125° to 190 kPa and 166°, respectively [4].

The motivation of this paper is to address the shortcomings pinpointed above. The hydrophilicity and hydrophobicity of membranes could be altered by changing the morphology of the surface via incorporation of nanoparticles. A facile method to produce the MD membrane with hydrophobic properties is possible by modifying the TiO_2 and controlling their distribution on the membrane surface.

2. Material and methods

2.1. Materials

Porous flat sheet membranes were fabricated from polyvinylidene fluoride, PVDF (Solef® TA6010, Solvay Solexis). The casting solutions were prepared by dissolving PVDF in N-methyl-2-pyrrolidone, NMP (Merck, Germany) (purity (GC) ≥99.5%). A commercial titanium dioxide (TiO_2) nanoparticle (Aeroxide P25) was obtained from Degussa.

2.2. Preparation of TiO_2 Suspension

TiO_2 nanoparticles were first chemically modified by adding 1M solution of hydrochloric acid (HCl) solution for 1 day. Then TiO_2 nanoparticles were collected by centrifugation and dried at 70 °C for a day in an oven. The same procedure was repeated by using 1 M of NaOH solution. After that, the modified particles were dried in an oven at 70 °C for 24 h and then cooled to room temperature in a vacuum chamber for 1h. The modified titanium oxide was then ground by using a mortar and pestle to reduce the number of large agglomerates. For this purpose, 5 g of modified titanium oxide was ground to fine powder. Afterward, the powder was dispersed in NMP by sonication in a sonication bath (Transconic 460 35 kHz, Germany) for 15 min. Samples treated by acid and alkali were labeled as Ac-TiO_2 and Al-TiO_2, respectively and the sample without treatment was labeled as U-TiO_2.

2.3. Membrane formation

The membrane casting solutions were prepared by dissolving pre-dried PVDF (24 hour oven drying at 70 °C) and using NMP as a solvent in a 200 mL beaker. It followed by adding 0.1 g of pre-dispersed modified/unmodified TiO_2 nanoparticles in NMP and sonicated for 15 min. Composition of the PVDF/NMP solutions was kept constant at 20:80 by weight percentage. The solution was prepared at 40 °C and stirred for 24 h to form a homogenous solution. Before casting, all the PVDF solution was cooled to room temperature in the incubator for 24 h. The polymer solution was then cast (at a nominal thickness of 200 µm) using a thin film applicator (Elcometer 4340) on a flat glass plate that was wrapped with tightly woven polyester fabric (Holleytex 3329, Ahlstrom). The nascent membrane was immediately immersed into the first isopropanol coagulation bath for 2 sec and then immersed into the second water coagulation bath (called dual coagulation method) for 24 h to allow the total solidification of the formed morphology as well as to remove the residual solvent. The formed membranes were further dried under ambient condition for 2 days [8, 12].

2.4. Surface morphology of membranes

The surface morphologies of PVDF/TiO_2 membranes were observed using SEM (Quanta Feg. 450). The membrane samples were first cut into an appropriate size and mounted on the sample holders. The membrane samples were then coated with a gold conducting layer to prevent the charge accumulation on the membrane surface.

2.5. Pore sizes and LEPw of membranes

The pore size of the membranes was determined using Capillary Flow Porometer Porolux 1000 (CNG Instruments). Membrane samples with a diameter of 10mm were characterized by using the "dry up–wet up" method. In this method, gas flow was measured as a function of trans-membrane pressure through the wetted membrane. The pressure of the gas was then increased gradually and the through-flow was recorded. When the pressure was sufficient to remove the liquid from the largest pores, the largest pore size (bubble point) was recorded. As pressure was increased, smaller pores become unblocked and the gas flow rate increased until the whole sample becomes dry. The cumulative pressure was used to calculate the average pore size. Non- cylindrical pores (such as those found in PVDF membranes) may have many diameters, but the wet/dry porometry technique measures only one diameter per pore, its smallest (throat) diameter. The pore sizes were estimated using perfluoroether (porefil) solution whereas the LEPw was evaluated using pure water and analyzed using PMI software.

2.6. Membrane wettability and porosity

The membrane wettability is characterized by a static contact angle of the membrane samples, which was measured, based on the sessile drop technique using a DropMeter A-100 contact angle system (Rame-Hart, U.S.A.). The membrane sample was stuck onto a glass slide using double-sided tape to ensure its top surface was upward and flat. A droplet (~13 µL) of deionized water was dropped onto the dry membrane surface using a microsyringe. Immediately, a microscope with long working distance 6.5×objectives was used to capture micrographs at high frequency (100 Pcs/s). The reported contact angles were average values from the measurements taken at 10 different locations on the membrane surface, as a measure to minimize random error.

For porosity measurement, the flat sheet PVDF membranes were cut into the dimension of 2×1 cm before immersing it in butanol (Merck) for 2 h. The membranes were weighed as wet membranes before being dried in the oven to eliminate any moisture in the membranes. The dry membranes were also weighed in order to calculate the porosity using the following equation:

$$\varepsilon = \frac{\frac{m_n}{\rho_n}}{\frac{m_n}{\rho_n} + \frac{m_p}{\rho_p}} \times 100\% \quad (1)$$

where ε is the porosity of the membrane, m_p is the mass of the dry membrane, m_n is the mass of the absorbed butanol, ρ_p is the density of the PVDF and ρ_n is the density of butanol. These parameters were used in determining the weight of liquid contained in the membrane pores. In this calculation, a total of five measurements were taken based on five different locations within the same membrane sample and the average value was taken [8].

2.7. Particle size analysis

Samples were prepared by mixing TiO_2 powders (0.01 g) and N-Methyl-2-pyrrolidone (200 mL), which were subjected to ultrasonic treatment for 10 min. The particle sizes of the samples were measured with particle size analysis equipment (Zeta Sizer, Malvern Co., U.K.).

2.8. Atomic force microscopy (AFM)

AFM (Model XE 100) was used to study the membrane surface roughness and topography via noncontact mode. Membranes with the size of 0.5×0.5 cm were fixed on a magnetic holder by using double-sided adhesive tape. All the AFM images were observed under room temperature. Scan areas (12.5×12.5 µm) were randomly selected from the surface. The roughness

parameters (root mean square) were determined.

2.9. Permeation flux and rejection measurements

A laboratory scale membrane distillation unit was used to study the permeation flux and rejection of the hydrophobic membrane by using 500 ml of nutrient broth as model solution. Nutrient solution consists of glucose, peptone, sodium bicarbonate, magnesium sulphate, monopotassium phosphate, dipotassium phosphate and calcium chloride [13]. The porous membrane with different morphology is tightly clamped between two acrylic plates, which divided the hot and cold flow streams. The hot stream is below the porous membrane while the cold stream is on top of it. The nutrient solution was circulated in the hot stream under an operating temperature of 50 °C, 60 °C, 70 °C, 80 °C and 90 °C. While in a cool site, the chiller temperature is kept constant at 19 °C. Both liquids are circulated in each cell by two independent pumps at atmospheric pressure. The feed velocity (0.5 LPM or 0.106 m/s) gave a laminar flow of R_e=595.50. The DCMD flux was calculated, in every case, by measuring the weight of condensate collected in the permeate chamber for a predetermined time. The experimental performances of the membrane are evaluated based on rejection and flux as shown in Eq. (2).

Rejection, R, is defined as:

$$R = \frac{C_f - C_p}{C_f} \times 100\% \quad (2)$$

where C_f and C_p denote the nutrient concentration based on COD measurement in feed and permeate, respectively.

The permeation flux of the membranes J is calculated by the following Eq. (3):

$$J = \Delta W / A.\Delta t \quad (3)$$

where J is the permeation flux ($kgm^{-2}h^{-1}$), ΔW is the quantity of distillate (kg), A is the effective inner surface area of the porous membranes (m^2) and Δt is the sampling time (h).

2.10. Antibacterial properties of membranes

The *B. Subtilis* microorganism was anaerobically grown in a sealed jar. The medium consisted of 5 g/l sodium chloride, 20 g/l peptone and 5 g/l K_2HPO_4. The medium was first sterilized in an autoclave at 15 psig and temperature of 121 °C for 20 min. The pH of the medium was adjusted to 7.1 and the inoculums were introduced into the media at ambient temperature. The inoculated cultures were incubated at 25-35 °C for the duration of 48 h [19, 20].

The membrane was cut into small pieces, rinsed with phosphate buffer saline (PBS) solution and then immersed in inoculated culture for 24 hours. The growth of bacteria formed on the membrane after 24 h served as an indicator for the biofouling phenomenon. After 24 hours, the membrane was rinsed with phosphate buffer saline (PBS) solution, 3% glutaraldehyde and dehydrating with a serial of ethanol solutions before scanning the image under SEM [16].

3. Result and discussions

3.1. Particle size distribution

The modified and unmodified nanoparticles were checked for particle size distribution in the NMP medium. Figure 1 shows the average particle size of U-TiO_2, Ac-TiO_2, and Al-TiO_2 in the NMP solvent. Due to the lower dielectric constant of NMP compared to water, the particles were seriously aggregated in the NMP medium. Nonetheless, it was found that the hydrodynamic size of Al-TiO_2 particles was smaller compared to the untreated TiO_2. This phenomenon is expected as alkaline modification did introduce an additional fixed charge (negative charge) on the particle surface. This is while in polar solvents (NMP) with a moderate dielectric constant, particles dispersed in such a medium can acquire charge and electrostatic forces that stabilize non aqueous suspensions via ionization. The increasing surface charge density provides stronger electrostatic repulsion which stabilizes the particles in the suspension. On the other hand, protonation occurs for acid treated TiO_2 which introduces positive charge to the surface. As a result, the originally negatively charged surface will be neutralized and cause particle aggregation due to the weakening electrostatic repulsion force.

3.2. Membranes physical properties

Figure 2 shows that the membranes exhibited an interconnected nodular structure. The linkage bridge observed in the fibril and stick-like elements between the nodules caused the membrane structure to become bicontinous (lacy) and resulted in high interconnectivity. These are expected morphology for the system with IPA as a soft non-solvent [17]. However, by adding the TiO_2, the membrane morphologies turned into a larger nuclei size with observable larger gaps between the nuclei. This phenomenon generates membranes with a larger effective pore size [18]. Table 1 shows that the pore size of the membrane with TiO_2 addition is almost doubled compared with the neat PVDF membrane. However, after adding the treated TiO_2 into the membrane, the distinctive nodules become less noticeable, probably due to the aggregation of the nodules and nanoparticles. Thus, instead of a bi-continuous structure, the membrane morphology changes to a structure that consisted of a large polymer domain. As a result, a slight decrease of porosity was observed for the TiO_2-PVDF membrane.

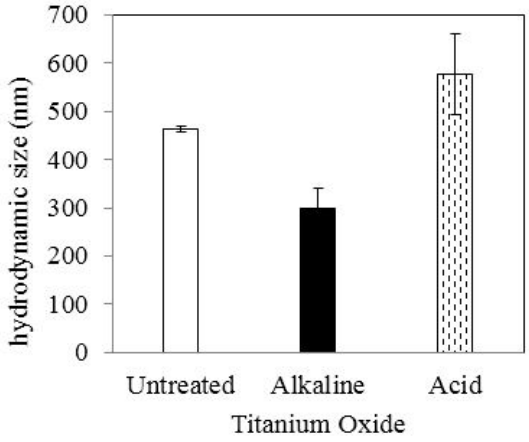

Fig. 1. Particle hydrodynamic size (Titanium Dioxide) in NMP.

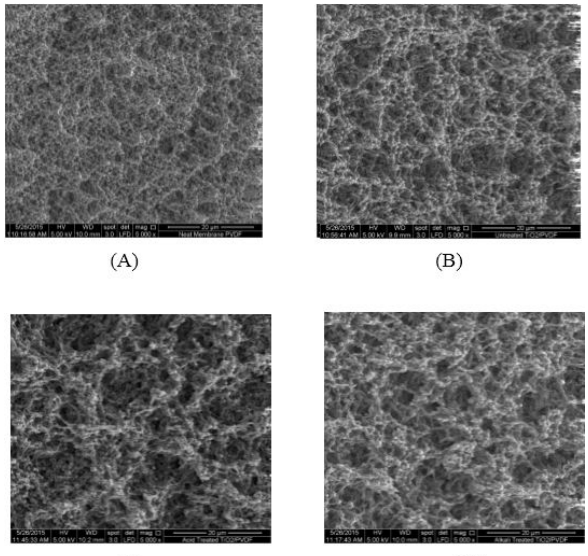

Fig. 2. SEM image of nanocomposite membrane with (A) neat membrane (B) U-TiO_2 (C) Ac-TiO_2 (D) Al-TiO_2 [Magnification: 5000x].

3.3. Membrane surface analysis

The surface energy of the membranes could be determined by measuring the water contact angle. Increasing contact angle implies the increase of membrane hydrophobicity. Figure 3 shows that the contact angle of the neat membrane is 120.2°. However, by incorporating the untreated TiO_2, the contact angle of the membrane slightly decreased to 112.3°. The same phenomenon was observed for acid treated TiO_2. However, for the case of the Al-TiO_2 membrane, the membrane with alkali modified TiO_2 exhibited an increment of contact angle which indicated that the membrane hydrophobicity was maintained. This phenomenon is due to the surface roughness

enhancement. The surface analysis was carried out using AFM to relate the surface roughness to the contact angle. Figure 3 demonstrates the three dimensional surface AFM images of the neat and TiO_2 modified PVDF membrane. In these images, the brightest area presents the highest point of the membrane surface and the dark regions indicate valley or membrane pores. The surface roughness parameters of the membrane were calculated based on the scan size of 12.5 µm × 12.5 µm. The mean roughness (R_a) of the neat PVDF-membrane and modified membrane (U-TiO_2, Ac-TiO_2 and Al-TiO_2) are 0.494 nm, 0.500 nm, 0.666 nm and 1.044 nm, respectively. Among these membranes, the Al-TiO_2 nanocomposite has the highest contact angle as well as highest surface roughness. The same phenomenon was reported by other researchers who found that the higher the surface roughness, the lower the surface energy or higher the contact angle [4, 19]. TiO_2 under alkali condition has a tendency to be negatively charged which resulted in strong repulsion with the negatively charged PVDF membrane. As a result, the tendency for the Al- TiO_2 to agglomerate was higher which led to the rougher membrane surface. Compared to the acid treated TiO_2 membrane, the alkaline treated TiO_2 membrane has a relatively protruding structure which contributes to the surface roughness.

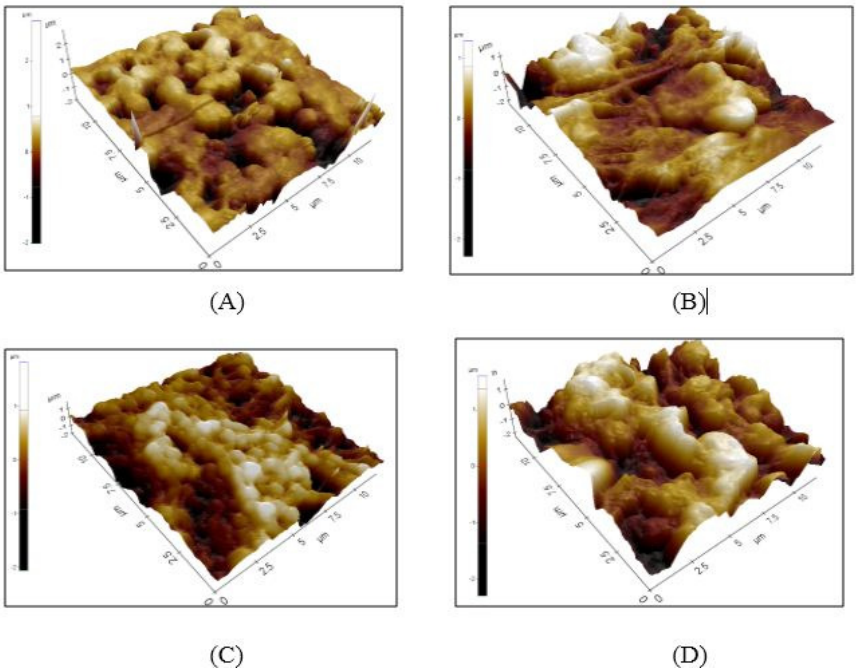

Fig. 3. AFM images of (A) neat PVDF membrane, (B) untreated-TiO_2-PVDF membrane, (C) Acid-treated-TiO_2-PVDF membrane and (D) Alkali treated-TiO_2-PVDF Membrane.

Table 1
Physical properties of the membranes.

Membrane	LEPw (bar)	Particle size distribution (nm)	Nominal Pore Size (um)	Porosity	Surface Roughness (Ra, µm)	Contact Angle (°)
PVDF	2.45±0.20	-	0.15±0.20	79.43%±1.15	0.494	120.2±3.76
U-TiO_2-PVDF	0.66±0.14	464.5±6.26	0.26±0.14	67.89%±1.51	0.500	112.3±2.52
Ac-TiO_2-PVDF	2.87±0.09	576.5±83.6	0.28±0.09	78.67%±1.45	0.666	115.5±2.65
Al-TiO_2-PVDF	2.98±0.09	298.7±41.4	0.24±0.09	78.72%±1.45	1.044	122±1.98

3.4. LEPw

Liquid-entry-pressure of water (LEPw), also called wetting pressure, is the pressure required for pure water to penetrate the membrane. For a membrane distillation, the LEPw value of the membrane should be high enough to prevent wetting. Table 1 shows the LEPw value of each membrane. It is clearly seen that although the membrane with the addition of TiO_2 has a larger pore size, the chemically modified TiO_2 nanocomposite membranes have higher LEPw of 2.98 bar and 2.87 bar for Al-TiO_2 and Ac-TiO_2, respectively. The trend of the LEPw again is in accordance with the contact angle. For the membrane with low surface energy, a higher force is required to push the water through the membrane pores. The drastic drops in LEPw of the U-TiO_2 membrane was mainly due to two reasons namely bigger pore size and lower contact angle. However, for Ac-TiO_2 and Al-TiO_2, even though the pore size became bigger, the LEPw was slightly higher. Based on the Laplace Equation, this phenomenon could only be explained by the changes of pore geometry coefficient to higher than unity. However, for the pore geometry coefficient, higher than unity is not possible. In that case, the Laplace equation could not be explicitly used to explain the LEPw and geometry relationship. The Laplace equation is more appropriate to be used to describe the partial wetting phenomenon. In this case, at such a high contact angle, the liquid is not penetrating due to the pillar effect. The contributing factor should therefore be attributed solely to the enhanced surface roughness.

3.5. Membrane performance

All these membranes were tested for membrane distillation at different feed temperatures. Direct contact membrane distillation (DCMD) configuration uses a cool water stream in the permeate side to create the vapor pressure difference through the membrane, which ultimately drives the separation process [10]. Figure 4 shows the flux profile for different feed inlet temperature by maintaining constant permeate temperatures. All the membranes showed higher flux at elevated temperature which was attributed by an increase of vapor pressure as depicted by the inserted images of Figure 4. For the same feed velocity (0.5 LPM or 0.106 m/s) and synthetic water concentration with COD value (2680 mg/L), the U-TiO_2 nanocomposite membrane recorded the lowest permeation flux. These phenomena could be attributed to two fold reasons namely pore wetting and low membrane porosity. As reported earlier, based on the LEPw and contact angle data, the membrane with U-TiO_2 is relatively more hydrophilic compared to the neat membrane. This will put the membrane with pore wetting phenomenon at risk and therefore reduce the effective driving force. Furthermore, the untreated TiO_2 membrane has the lowest porosity (67.89%±1.51) that gives

higher water permeation resistance.

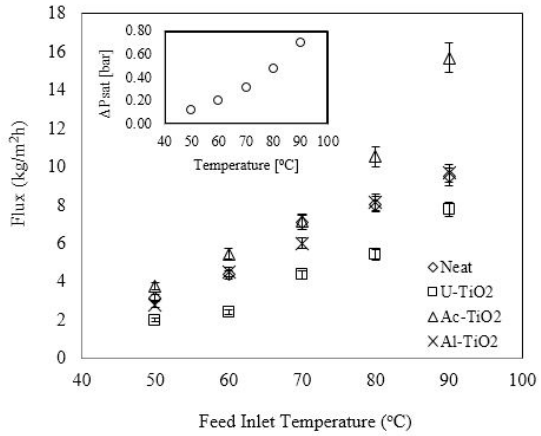

Fig. 4. Membrane flux as a function of feed temperature.

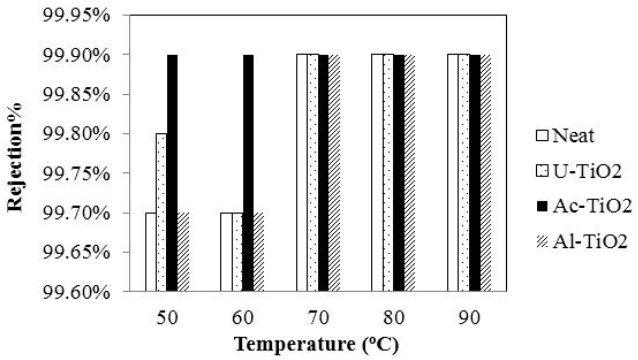

Fig. 5. Percentage of Rejection for different membranes.

On the other hand, the Ac-TiO_2 has the highest flux amongst the membranes, especially at higher feed temperature. Amongst the membranes, the Ac-TiO_2 membrane has relatively bigger pore size and reasonably high porosity which exerts minimum flow resistance to the vapor, and as a result, higher water permeation could be achieved. As the flux of the membrane is proportional to the vapor pressure driving force, the membrane that is not pore wetted should have an exponential flux profile over the increasing temperature (as shown in the inset ΔP_{sat}-T graph). In this case, the Ac-TiO_2-PVDF membrane showed a similar exponential profile, therefore, it can be concluded that the Ac-TiO_2 membrane showed substantial resistance to membrane wetting.

Figure 5 shows the rejection profile of the membranes at different temperatures. All membranes had COD rejection of more than 99.6%. The Ac-TiO_2-PVDF membrane shows a stable rejection performance compared to others even at lower operating temperature. This effect was mainly due to the hydrophobic nature of the membrane which resists permeation of nutrients through the membrane and water is the only volatile component in the feed that passes through.

3.6. Antibacterial properties of TiO2 entrapped PVDF membranes

The purpose of TiO_2 inclusion is to enhance the membrane antibacterial properties. Bacteria fouling on both the pristine and nanocomposite membrane were investigated. SEM images taken after the PVDF flat sheet membranes were exposed to *B. Subtilis* for 24 hours. The SEM images (see Figure 6) show that the pristine PVDF membrane was seriously fouled by *B. Subtilis* bacteria. Bacterial cells adhered readily to the membrane surfaces and a stack forms in the clusters. In comparison, the TiO_2 nanocomposite membranes showed almost a bacteria free surface, suggesting significant antibacterial properties of the composite membrane. Since the contact angles of the pristine membrane are not much different from the nanocomposite membrane, we can rule out the effect of surface energy in preventing the adhesion of bacteria. The only plausible reason is that TiO_2 possesses the antibacterial effect even with the absence of UV light [20]. The presence of nanoparticles gave surface stress to the bacteria that prevents bacteria growth on the surface.

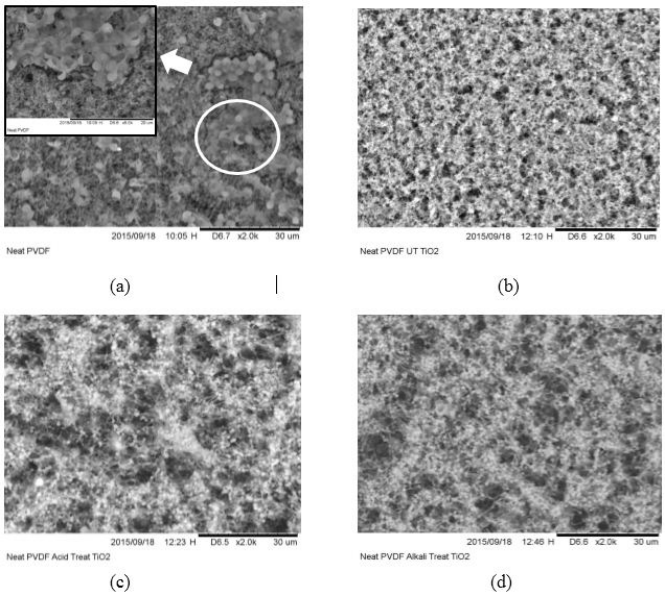

Fig. 6. SEM images of membrane surface after *B. Subtilis* incubation. (a) Neat PVDF, (b) U-TiO_2 PVDF Membrane, (c) Ac-TiO_2 PVDF Membrane, (d) Al-TiO_2 PVDF Membrane.

4. Conclusion

The PVDF membrane modified with TiO_2 nanoparticles exhibited desirable antibacterial properties that make it very suitable for membrane distillation applications. The addition of untreated TiO_2 nanoparticles into the polymer matrix resulted in lower membrane porosity as well as low LEPw value. However, by modifying the nanoparticles with acid or alkali, the porosity and LEPw of the membranes are increased. The increasing LEPw was due to the surface roughness enhancement. Furthermore, due to the bigger pore size, large porosity as well as high LEPw, the acid-treated TiO_2-PVDF membrane exhibited the highest permeation flux and stable nutrient isolation. The results of the antibacterial study indicated that the TiO_2 modified membranes had significant antibacterial (*B. Subtilis*) properties even with the absence of UV light. By incorporating acid/alkali modified TiO_2 into the PVDF membrane matrix, the hydrophilization effect could be solved with concomitant antibacterial properties.

Acknowledgements

The authors gratefully acknowledge the financial support from Universiti Sains Malaysia (USM) Research University Grant (1001/PJKIMIA/814210), USM Membrane Science and Technology Cluster and University Malaysia Perlis (SLAI 2013) for financial supports throughout the study.

References

[1] J. Zhao, M. Milanova, M.M.C.G. Warmoeskerken, V. Dutschk, Surface modification of TiO_2 nanoparticles with silane coupling agents, Colloids Surfaces A Physicochem. Eng. Asp. 413 (2012) 273-279.
[2] L. Yan, Y.S. Li, C.B. Xiang, S. Xianda, Effect of nano-sized Al_2O_3-particle addition on PVDF ultrafiltration membrane performance, J. Membr. Sci. 276 (2006) 1818-1821.
[3] J. Du, L. Wu, C.Y. Tao, C.X. Sun, Preparation and characterization of Fe3O4/PVDF magnetic composite membrane, Acta Phys. - Chim. Sin. 20 (2004) 598–601.
[4] A. Razmjou, E. Arifin, G. Dong, J. Mansouri, V. Chen, Superhydrophobic modification of TiO2 nanocomposite PVDF membranes for applications in membrane distillation, J. Memb. Sci. 415-416 (2012) 850–863.
[5] X. Zhang, Y. Wang, Y. You, H. Meng, J. Zhang, X. Xu, Preparation, performance and adsorption activity of TiO_2 nanoparticles entrapped PVDF hybrid membranes, Appl. Surf. Sci. 263 (2012) 660–665.
[6] A. Rahimpour, M. Jahanshahi, B. Rajaeian, M. Rahimnejad, TiO_2 entrapped nano-composite PVDF/SPES membranes: Preparation, characterization, antifouling and antibacterial properties, Desalination 278 (2011) 343–353.
[7] R.A. Damodar, S.-J. You, H.-H. Chou, Study the self-cleaning, antibacterial and photocatalytic properties of TiO2 entrapped PVDF membranes. J. Hazard. Mater. 172 (2009) 1321–1328.
[8] A.L. Ahmad, W.K.W. Ramli, Hydrophobic PVDF membrane via two-stage soft coagulation bath system for Membrane Gas Absorption of CO2, Sep. Purif. Technol.

103 (2013) 230–240.
[9] H.Y. Wu, R. Wang, R.W. Field, Direct contact membrane distillation: An experimental and analytical investigation of the effect of membrane thickness upon transmembrane flux, J. Memb. Sci. 470 (2014) 257–265.
[10] N. Pezeshk, R.M. Narbaitz, More fouling resistant modified PVDF ultrafiltration membranes for water treatment, Desalination. 287 (2012) 247–254.
[11] J.F. Li, Z.L. Xu, H. Yang, L.Y. Yu, M. Liu, Effect of TiO2 nanoparticles on the surface morphology and performance of microporous PES membrane, Appl. Surf. Sci. 255 (2009) 4725–4732.
[12] H.P. Ngang, B.S. Ooi, A.L. Ahmad, S.O. Lai, Preparation of PVDF–TiO2 mixed-matrix membrane and its evaluation on dye adsorption and UV-cleaning properties, Chem. Eng. J. 197 (2012) 359–367.
[13] J. Phattaranawik, A.G. Fane, A.C.S. Pasquier, W. Bing, A novel membrane bioreactor based on membrane distillation, Desalination 223 (2008) 386–395.
[14] H. Fujikawa, Periodic growth of Bacillus subtilis colonies on agar plates, Phys. A Stat. Mech. Its Appl. 189 (1992) 15–21.
[15] A. Arunachalam, S. Dhanapandian, C. Manoharan, G. Sivakumar, Physical properties of Zn doped TiO2 thin films with spray pyrolysis technique and its effects in antibacterial activity. Spectrochim. Acta. A. Mol. Biomol. Spectrosc. 138 (2015) 105–12.
[16] X. Li, T. Cai, T.-S. Chung, Anti-Fouling Behavior of Hyperbranched Polyglycerol-Grafted Poly(ether sulfone) Hollow Fiber Membranes for Osmotic Power Generation., Environ. Sci. Technol. 48 (2014) 9898–907.
[17] A.L. Ahmad, N. Ideris, B.S. Ooi, S.C. Low, A. Ismail, Morphology and polymorph study of a polyvinylidene fluoride (PVDF) membrane for protein binding: Effect of the dissolving temperature, Desalination 278 (2011) 318–324.
[18] A. Razmjou, J. Mansouri, V. Chen, The effects of mechanical and chemical modification of TiO2 nanoparticles on the surface chemistry, structure and fouling performance of PES ultrafiltration membranes, J. Memb. Sci. 378 (2011) 73–84.
[19] S. Giljean, M. Bigerelle, K. Anselme, H. Haidara, New insights on contact angle/roughness dependence on high surface energy materials, Appl. Surf. Sci. 257 (2011) 9631-9638.
[20] Y. Cai, M. Strømme, K. Welch, Photocatalytic antibacterial effects are maintained on resin-based TiO_2 nanocomposites after cessation of UV irradiation, PLoS One. 8 (2013) e75929.